

# Multigenerational maternal obesity increases the incidence of HCC in offspring via miR-27a-3p

Yu Sun<sup>1</sup>, Qing Wang<sup>1</sup>, Yu Zhang<sup>2</sup>, Mengyuan Geng<sup>1</sup>, Yujuan Wei<sup>2</sup>, Yanrui Liu<sup>1</sup>, Shanshan Liu<sup>1</sup>, Robert B. Petersen<sup>3</sup>, Junqiu Yue<sup>4</sup>, Kun Huang<sup>2,\*</sup>, Ling Zheng<sup>1,5,\*</sup>

<sup>1</sup>Hubei Key Laboratory of Cell Homeostasis, College of Life Sciences, Wuhan University, Wuhan, China, 430072; <sup>2</sup>Tongji School of Pharmacy, Tongji Medical College, Huazhong University of Science and Technology, Wuhan, China, 430030; <sup>3</sup>Foundational Sciences, Central Michigan University College of Medicine, Mt. Pleasant, MI, USA, 48858; <sup>4</sup>Department of Pathology, Hubei Cancer Hospital, Tongji Medical College, Huazhong University of Science and Technology, Wuhan, China, 430030; <sup>5</sup>Frontier Science Center for Immunology and Metabolism, Wuhan University, Wuhan, China, 430072

**Background & Aims:** Obesity is an independent risk factor for malignancies, including hepatocellular carcinoma (HCC). However, it remains unknown whether maternal obesity affects the incidence of HCC in offspring. Thus, we aimed to investigate this association and its underlying mechanisms.

**Methods:** Diethylnitrosamine (DEN) was used to induce HCC in a high-fat diet (HFD)-induced multigenerational obesity model. RNA-sequencing was performed to identify the genes and microRNAs (miRNAs) that were altered over generations. The role of the miR-27a-3p-Acs1/Aldh2 axis in HCC was evaluated in cell lines and HCC-bearing nude mice, and its intergenerational impact was studied in pregnant mice and their offspring.

**Results:** Under HFD stress, maternal obesity caused susceptibility of offspring to DEN-induced HCC, and such susceptibility was cumulative over generations. We identified that *Acs1* and *Aldh2*, direct targets of miR-27a-3p, were gradually changed over generations. Under hyperlipidemic conditions, downregulation of *Acs1* and *Aldh2* increased cell proliferation (*in vitro*) or tumor growth (*in vivo*) in synergy. Intratumor injection of an miR-27a-3p agomir exacerbated tumor growth by downregulating *Acs1* and *Aldh2*; while intratumor injection of an miR-27a-3p antagonist had the opposite effect. Moreover, serum miR-27a-3p levels gradually increased in the HFD-fed maternal lineage over generations. Injecting pregnant mice with an miR-27a-3p agomir not only upregulated hepatic miR-27a-3p and downregulated *Acs1/Aldh2* in offspring (fetus, young and adult stages), but also exacerbated HCC development in DEN-treated offspring. In human HCC, upregulated miR-27a-3p and downregulated *Acs1/Aldh2* were negatively correlated with survival on TCGA analysis; while, hepatic miR-27a-3p was negatively correlated with *Acs1/Aldh2* expression in tumor/non-tumor tissues from fatty/non-fatty livers.

**Conclusions:** Maternal obesity plays a role in regulating cumulative susceptibility to HCC development in offspring over multiple generations through the miR-27a-3p-Acs1/Aldh2 axis.

**Lay summary:** It is not currently known how maternal obesity affects the incidence of liver cancer in offspring. In this study, we identified a microRNA (miR-27a-3p) that was upregulated in obese mothers and could be passed on to their offspring. This microRNA enhanced the risk of liver cancer in offspring by regulating 2 genes (*Acs1* and *Aldh2*). This mechanism could be a future therapeutic target.

© 2020 European Association for the Study of the Liver. Published by Elsevier B.V. All rights reserved.

## Introduction

One-third of the population are overweight or obese; epidemiological studies suggest that obesity is an independent risk factor for malignant tumors such as colon cancer, breast cancer, and liver cancer.<sup>1</sup> For example, obesity increases the odds of developing liver cancer by 1.5–4.0 fold<sup>2</sup>; a 16-year prospective study of 900,000 Americans found that the incidence of liver cancer in obese men and women was 4.52- and 1.68-fold higher than that in non-obese individuals.<sup>3</sup>

Up to 50% of recently diagnosed HCC in the USA is the result of hepatic metabolic disorders such as non-alcoholic fatty liver disease (NAFLD).<sup>4</sup> Maternal obesity, which directly affects the health of offspring, plays a critical role in the obesity epidemic and metabolic diseases.<sup>5,6</sup> Offspring of obese mothers are at increased risk of developing metabolic diseases, including NAFLD, independent of the body weight of their fathers, indicating that maternal factors play a major role in the inheritance of obesity.<sup>7</sup> We previously demonstrated that the offspring of mothers exposed to high-fat diet (HFD) stress over multiple generations showed gradual increases in obesity and NAFLD score.<sup>8</sup> However, whether the offspring of obese mothers are more prone to develop malignant tumors, such as HCC, is currently unknown.

Epigenetic mechanisms are involved in multigenerational obesity.<sup>8,9</sup> Growing evidence suggests that non-coding RNAs mediate heritable phenotypes in their offspring,<sup>10</sup> for example, maternal circulating microRNAs (miRNAs) have been suggested to cross the placenta and affect the phenotype of

Keywords: Intergenerational effects; Maternal obesity; Hepatocellular carcinoma; miR-27a-3p; *Acs1*; *Aldh2*; MicroRNA.

Received 11 October 2019; received in revised form 19 March 2020; accepted 20 March 2020; available online xxx

\* Corresponding authors. Addresses: College of Life Sciences, Wuhan University, Wuhan, China, 430072. Tel.: 86-27-68755559, fax: 86-27-68755559 (L. Zheng), or Tongji School of Pharmacy, Huazhong University of Science and Technology, Wuhan, China, 430030. Tel.: 86-27-83692921, fax: 86-27-83692921 (K. Huang).

E-mail addresses: lzheng@whu.edu.cn (L. Zheng), kunhuang@hust.edu.cn (K. Huang).  
<https://doi.org/10.1016/j.jhep.2020.03.050>



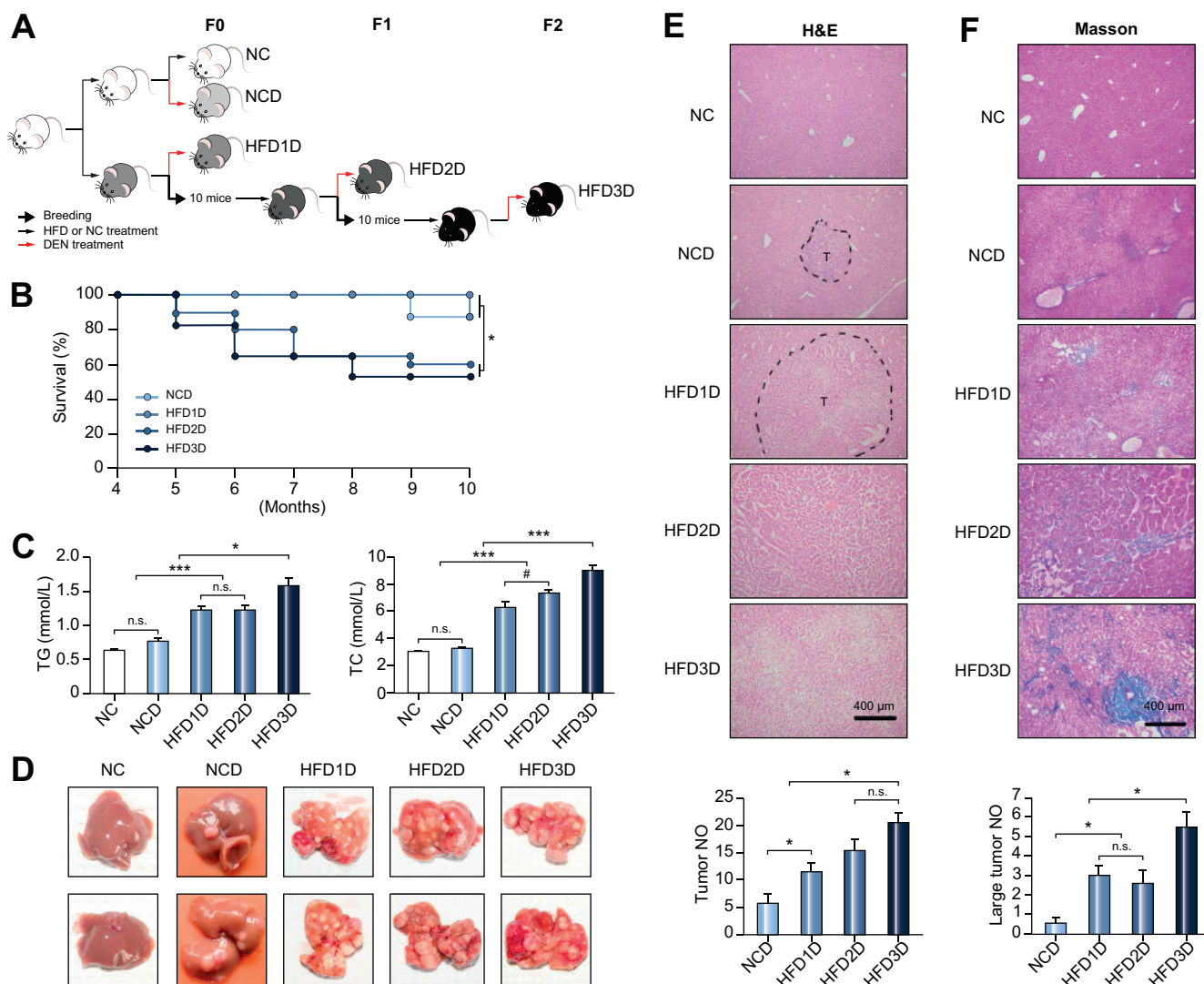


**Fig. 1. Maternal exposure to multigenerational HFD stress gradually increases susceptibility to HCC in their offspring.** (A) Experimental design flowchart of DEN-induced HCC in mice with multigenerational HFD-feeding stress. NC-fed mice, white; DEN-treated NC-fed mice, light grey; DEN-treated HFD-fed mice, grey for HFD1D, dark grey for HFD2D, and black for HFD3D. (B) Survival ratio of DEN-injected offspring with multigenerational HFD-feeding stress.  $n = 8, 8, 20$  and  $17$  for NCD, HFD1D, HFD2D and HFD3D group;  $*p < 0.05$  (Mann-Whitney  $U$  test). (C) Serum TG and TC levels. Data shown as mean  $\pm$  SEM.  $n = 6, 7, 7, 12$  and  $9$  for NC, NCD, HFD1D, HFD2D and HFD3D group;  $*p < 0.05$ ;  $***p < 0.001$ ;  $\#p = 0.08$ ; n.s., not significant (Mann-Whitney  $U$  test). (D) Two representative liver pictures for each group, and quantification results of tumor and large tumor number; Data shown as mean  $\pm$  SEM.  $n = 4, 7, 7, 12$  and  $9$  for NC, NCD, HFD1D, HFD2D and HFD3D group;  $*p < 0.05$ ; n.s., not significant (Mann-Whitney  $U$  test). (E-F) Representative pictures for H&E (E) and Masson (F) stained liver sections ( $n = 4, 7, 7, 8$  and  $8$  for NC, NCD, HFD1D, HFD2D and HFD3D group). Dotted lines indicate the outline of tumors. Scale bar,  $400 \mu\text{m}$ . DEN, diethylnitrosamine; HCC, hepatocellular carcinoma; HFD, high-fat diet; NC, normal chow; NCD, normal chow + DEN; HFD(1/2/3)D, (F0/1/2) male offspring under high-fat diet + DEN; TC, total cholesterol; TG, triglyceride.

offspring.<sup>11,12</sup> However, the links between maternal non-coding RNAs and disease development in offspring have not been established.

Herein, we studied the susceptibility of offspring from obese mothers to diethylnitrosamine (DEN)-induced HCC under HFD stress, using a previously reported mouse model.<sup>8,13</sup> Multigenerational changes in miRNAs and genes in the livers of offspring were identified by RNA-sequencing. Furthermore, using database and clinical samples, tumor xenografts, cultured cells and mouse models, we demonstrated an epigenetic mechanism operating intergenerationally via the miR-27a-3p-Acsl1/Alhd2 axis, which has a role in regulating the HCC incidence of offspring from obese mothers.

## Materials and methods

### Mice, diets, and experimental design

C57BL/6 breeding pairs were from Hubei Center for Disease Control and Prevention. Male BALB/c nude mice were from Hunan SJA Animal Laboratory. Animals were handled according to the Guidelines of the China Animal Welfare Legislation as approved by the Committee on Ethics in the Care and Use of Laboratory Animals, College of Life Sciences, Wuhan University.

The experimental design used to study HCC susceptibility in the offspring of multigenerational HFD-stressed mothers is shown (Fig. 1A). Briefly, female mice (F0 generation) were fed normal chow (NC) or HFD (60% kcal fat; Research Diets, New Brunswick, NJ) from 1 month to 3 months old, and mated with

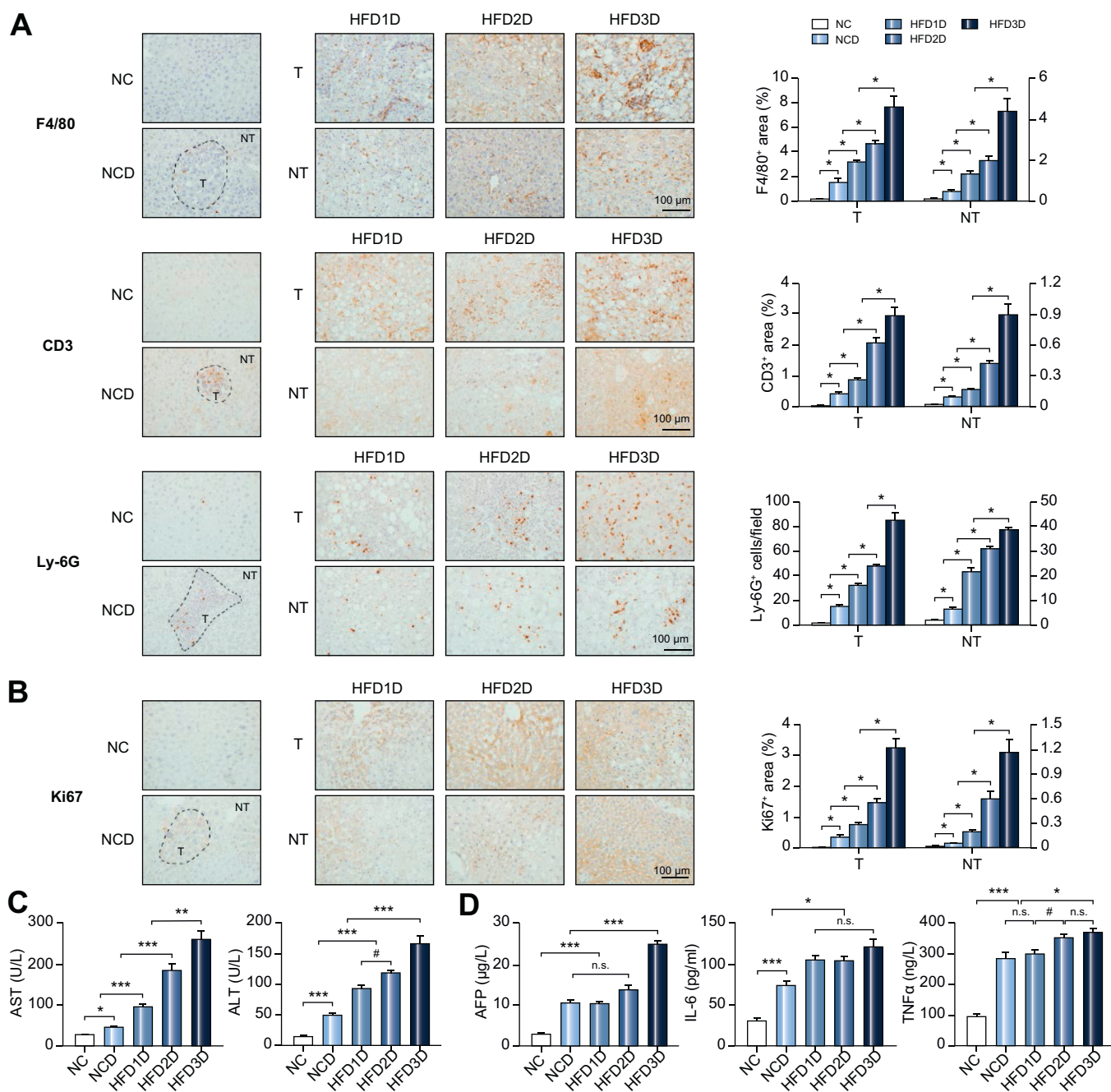


**Fig. 2. Maternal exposure to multigenerational HFD stress gradually increases hepatic inflammation and proliferation of their offspring.** (A–B) Representative pictures for F4/80, CD3 and Ly-6G staining with quantification results (A), and Ki67 staining with quantification results (B). Data shown as mean  $\pm$  SEM.  $n = 4, 5, 5, 5$  and  $5$  for NC, NCD, HFD1D, HFD2D and HFD3D group; \* $p < 0.05$  (Mann-Whitney  $U$  test); scale bar,  $100 \mu\text{m}$ ; dotted lines indicate the outline of tumors. (C) Quantification results of serum AST and ALT levels. Data shown as mean  $\pm$  SEM.  $n = 6, 7, 7, 12$  and  $9$  for NC, NCD, HFD1D, HFD2D and HFD3D group; \* $p < 0.05$ ; \*\*\* $p < 0.001$ ; # $p = 0.08$  (Mann-Whitney  $U$  test). (D) Quantification results of serum AFP, IL-6 and TNF $\alpha$  levels. Data shown as mean  $\pm$  SEM.  $n = 6, 6, 7, 9$  and  $8$  for NC, NCD, HFD1D, HFD2D and HFD3D group; \* $p < 0.05$ ; \*\*\* $p < 0.001$ ; # $p = 0.08$ ; n.s., not significant (Mann-Whitney  $U$  test). AFP, alpha-fetoprotein; ALT, alanine aminotransferase; AST, aspartate aminotransferase; HFD, high-fat diet; IL-, interleukin; NC, normal chow; NCD, normal chow + diethylnitrosamine; HFD(1/2/3)D, (F0/1/2) male offspring under high-fat diet + diethylnitrosamine; TC, total cholesterol; TG, triglyceride; TNF $\alpha$ , tumor necrosis factor- $\alpha$ .

NC-fed male mice to breed the F1 generation as we previously reported.<sup>8</sup> The F2 generation was similarly created. Male mice of the F0, F1 and F2 generations were injected intraperitoneally with DEN (25 mg/kg body weight; Sigma, Saint Louis, MO) at p15 as previously reported,<sup>14</sup> and maintained on HFD after weaning which were named HF1D, HF2D or HF3D group, respectively

(Fig. 1A). Meanwhile, male mice of the F0 generation injected with either PBS (NC group) or DEN (NCD group) at the same age and maintained on NC were used as the control groups. All groups were sacrificed at 40 weeks of age. The incidence of HCC was determined by counting tumors (tumors with diameters of 2–8 mm are designated 'tumor'; diameter  $> 8$  mm are designated

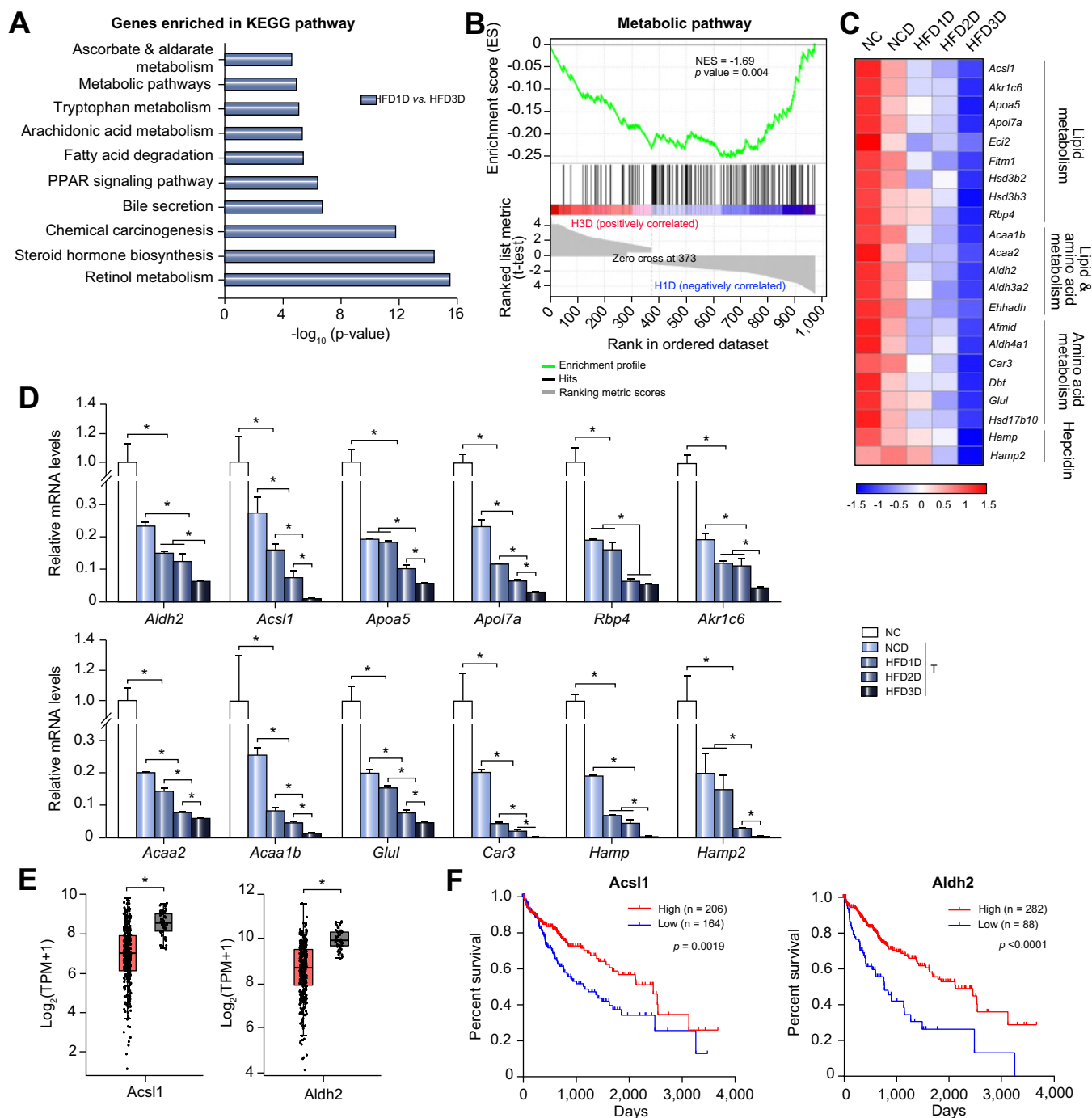


**Fig. 3. Identification of genes gradually altered in tumors of male offspring over generations.** (A) Top 10 KEGG pathways that show differentially expressed genes enriched between HFD1D and HFD3D. (B) Gene enrichment analysis in metabolic pathway (data analyzed with *t* test). (C) Heatmap of different gene identified from RNA-sequencing analysis in NC, NCD, HFD1D, HFD2D and HFD3D groups. (D) qPCR validations. Gene expression normalized to actin. Data shown as mean  $\pm$  SEM. n = 4 per group; \**p* < 0.05 (Mann-Whitney *U* test). (E) *Acs1* and *Aldh2* levels in tumor and normal tissue of patients with HCC. Tumor (red, n = 369); normal (grey, n = 50); \**p* < 0.05 (ANOVA). (F) Survival ratio of patients with HCC and different expression levels of *Acs1* and *Aldh2*. Data were analyzed with log-rank test. HCC, hepatocellular carcinoma; HFD, high-fat diet; NC, normal chow; NCD, normal chow + diethylnitrosamine; HFD(1/2/3)D, (F0/1/2) male offspring under high-fat diet + diethylnitrosamine.

'large tumor') under dissecting microscope. Serum, tumor (diameter > 2 mm) and non-tumor tissues were collected for further analysis.

In another set of experiments, multiple generations of HFD-fed mothers, named NCF, HF1F and HF2F group, were created (Fig. S1) and sacrificed at 16 weeks of age. Serum was collected.

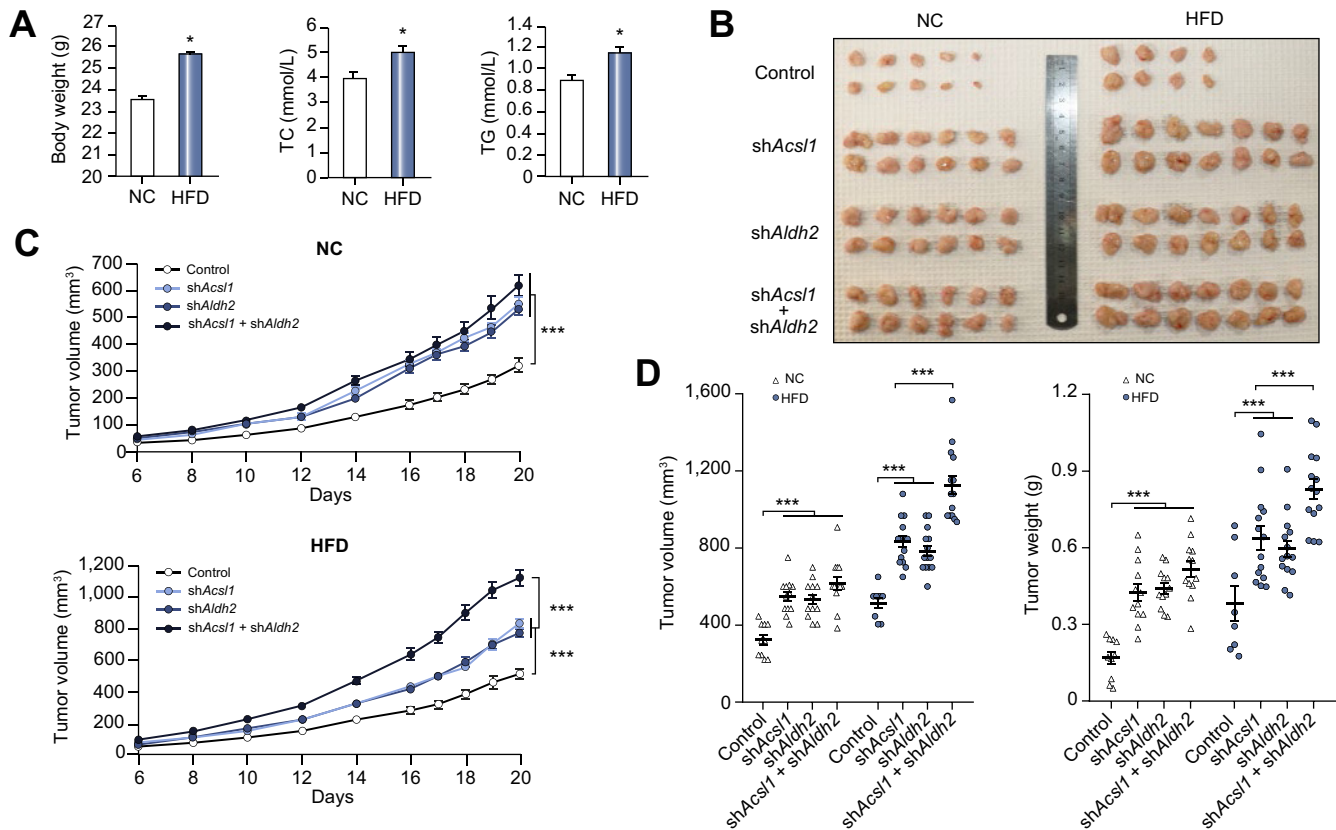


**Fig. 4. Knockdown of Acs1 and Aldh2 promotes cell proliferation in xenograft tumor experiment.** (A) Body weight, serum TC and TG levels of nude mice fed with NC or HFD. Data shown as mean  $\pm$  SEM.  $n = 23$  and  $25$  for body weight of NC and HFD-fed nude mice,  $n = 6$  per group for TC and TG measurements; \* $p < 0.05$  (Mann-Whitney  $U$  test). (B–D) Isolated tumors (B), growth curve (C), volume (left) and weight (right) (D) of xenograft tumor of different groups fed with NC or HFD. Data shown as mean  $\pm$  SEM.  $n = 10, 12, 12$  and  $12$  for NC-fed nude mice injected with CT, shAcs1, shAldh2 and shAcs1 + shAldh2;  $n = 8, 14, 14$  and  $14$  for HFD-fed nude mice injected with CT, shAcs1, shAldh2 and shAcs1 + shAldh2; \*\*\* $p < 0.001$  (Mann-Whitney  $U$  test). CT, control; HFD, high-fat diet; NC, normal chow; shRNA, short hairpin RNA; TC, total cholesterol; TG, triglyceride.

#### miRNA agomir injection for pregnant mice

Pregnant C57BL/6 females were injected in the tail vein with PBS or an agomir of miR-27a-3p (miR40000537, synthesized by RiboBio;  $5 \mu\text{mol}$  per mouse at E12.5 and  $3 \mu\text{mol}$  per mouse every other day, E14.5 to E18.5). The livers from E14.5 fetuses, p1, p5, and p15 pups were collected. DEN was injected intraperitoneally into p15 male offspring, which were maintained on NC or HFD after weaning, named as Control+NC, Agomir+NC, Control+HFD and Agomir+HFD group, respectively. NC-fed males were used as controls. All groups were sacrificed at 32 weeks of age. Serum and tumors were collected.

#### Measurements of serum factors and miRNAs

Serum levels of alanine aminotransferase (ALT), aspartate aminotransferase (AST), total cholesterol (TC), triglyceride (TG), interleukin (IL)-6, tumor necrosis factor- $\alpha$  (TNF $\alpha$ ) and alpha-fetoprotein (AFP) were measured using ALT/AST kits (Jiancheng, Nanjing, China), total cholesterol or triglyceride kit (KeHua, Shanghai, China), IL-6, TNF $\alpha$  or AFP ELISA Kits (FanKe, Shanghai, China).

Serum RNA was extracted using a miRNeasy Kit (QIAGEN, Germany). One microgram of RNA from each sample was reverse transcribed into cDNA using miRNA qPCR Starter Kit (C10712, RiboBio). qPCR was performed with specific primers synthesized

(RiboBio) for the targeted miRNA. Equal amounts of cel-miR-67-3p were added before RNA extraction as the external control.

#### Histological, immunohistochemical and *in situ* hybridization staining

Mouse liver samples were embedded in paraffin and sectioned. Liver paraffin sections from 54 patients with HCC were obtained from the Affiliated Hubei Cancer Hospital, with informed consent and approval by the Ethics Committee of the Affiliated Hubei Cancer Hospital in accordance with the principle of the Helsinki Declaration. For histological evaluation, H&E or Masson's trichrome staining were performed.<sup>15,16</sup> For immunohistochemical staining, sections were incubated overnight with primary antibodies (Table S2) and visualized by DAB substrate (Vector laboratories). For miR-27a-3p *in situ* hybridization staining, miRNA ISH Optimization Kit (339455, QIAGEN) and hsa-miR-27a-3p miRNA detection probe (339111, QIAGEN) were used.

#### Sequencing of long non-coding RNA and small RNA

Total RNA of tumor samples from different groups (40-week-old male offspring) was extracted individually using RNAiso Plus (Takara Biotechnology). An equal amount of RNA ( $n = 4-8$ ) from the same group was combined into 2 samples/group for long non-coding RNA-sequencing and 1 sample/group for small RNA-sequencing as described previously.<sup>13,17</sup> Sequencing was

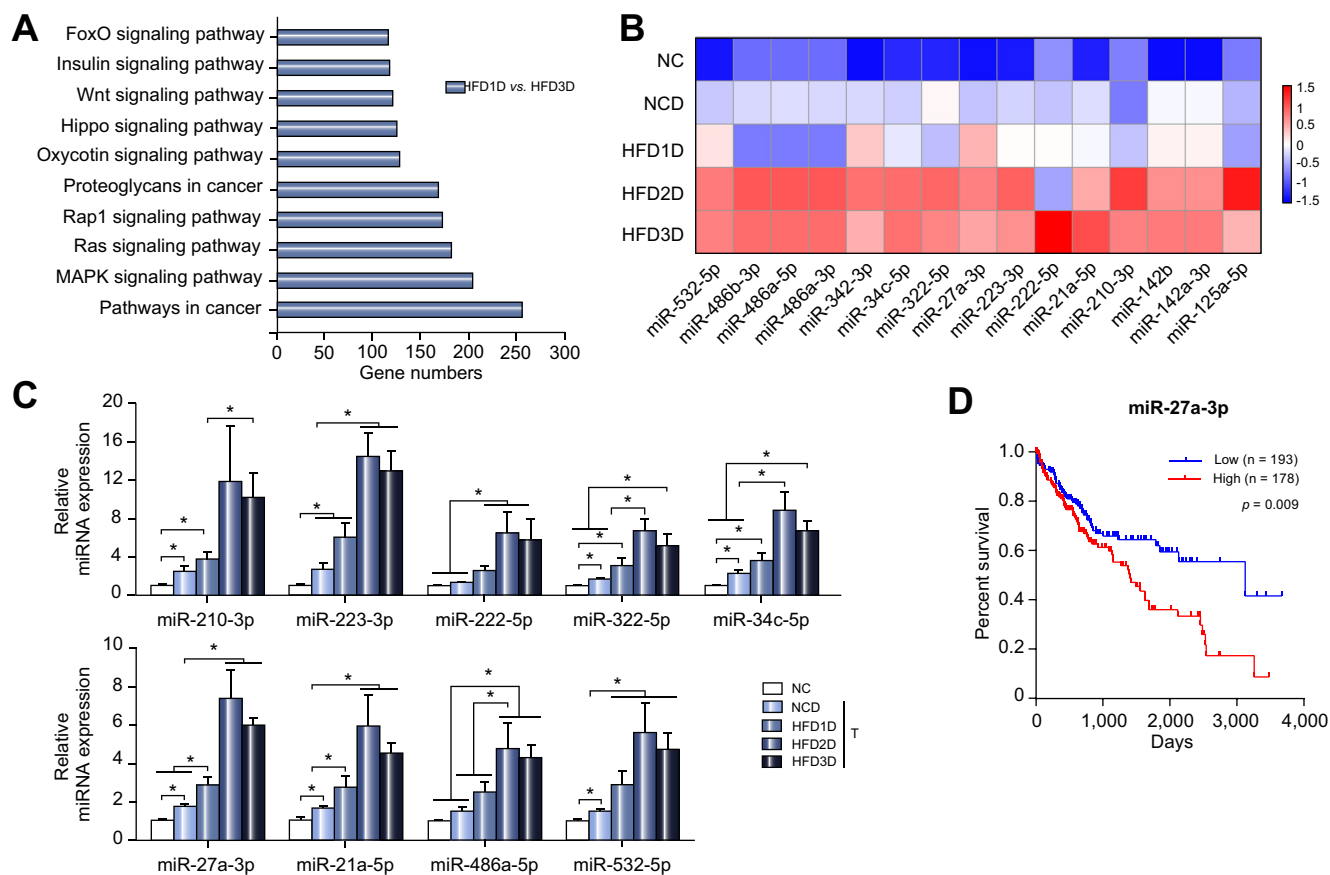


**Fig. 5. Identification of miRNAs gradually altered in tumor of male offspring over generations.** (A) Top 10 KEGG pathways that are differentially expressed between HFD1D and HFD3D. (B) Heatmap of miRNAs gradually altered in NC, NCD, HFD1D, HFD2D and HFD3D groups, identified by RNA-sequencing analysis. (C) Validation of miRNAs by qPCR. miRNA expression was normalized to miR-340-3p. Data shown as mean  $\pm$  SEM.  $n = 4, 5, 5, 5$  and  $5$  for NC, NCD, HFD1D, HFD2D and HFD3D groups; \* $p < 0.05$  (Mann-Whitney  $U$  test). (D) Survival ratio of patients with HCC and different hepatic levels of miR-27a-3p. Data were analyzed with log-rank test. HCC, hepatocellular carcinoma; HFD, high-fat diet; miRNA, microRNA; NC, normal chow; NCD, normal chow + diethylnitrosamine; HFD(1/2/3)D, (F0/1/2) male offspring under high-fat diet + diethylnitrosamine.

performed by Novogene (Beijing, China) with details provided in the [supplementary methods](#).

### Cell culture, plasmids, and transfection

HCC cell lines HepG2 (human) and Hepa1-6 (mouse) were obtained from China Center for Type Culture Collection (CCTCC, GDC024) and Rothen Pharma (CL-433), respectively. To knock-down *Acs11* or *Aldh2*, HepG2 cells were transfected with either a scrambled short hairpin RNA (shRNA) or an shRNA targeting *Acs11* or *Aldh2* (Table S1); stable knockdown cell lines were obtained by puromycin selection.<sup>14,18</sup> To create an *Acs11* and *Aldh2* double-knockdown (sh*Acs11*+sh*Aldh2*) stable cell line, the *Aldh2* stable knockdown cells were transfected with lentivirus packed sh*Acs11* plasmid twice (24 h apart), and selected with puromycin.

Human-specific Hsa-miR-27a-3p mimic (miR10000084-1-5) or inhibitor (miR20000084-1-5) and mouse specific mmu-miR-27a-3p mimic (miR10000537-1-5) or inhibitor (miR20000537-1-5), all synthesized by RiboBio, were transfected into HepG2 cells or Hepa1-6 cells, respectively, using a Transfection Kit (C10511-1, RiboBio). Cells transfected with micrON mimic (miR01201-1-5) or micrOFF inhibitor (miR02201-1-5) were used as respective controls.

### Luciferase reporter assays

The siCHECK2 luciferase reporter for 3' UTR-WT (wild-type) or 3' UTR-mut (mutant, miR-27a-3p binding core bases mutated to A) of mouse *Acs11* and *Aldh2* were constructed (Table S1). Twelve hours after transfection of mmu-miR-27a-3p mimic, or inhibitor, or control micrON mimic, plasmids for luciferase reporter assays were individually transfected. Twenty-four hours later, luciferase activities were measured as described.<sup>19</sup>

### MTT and colony formation

HepG2 or Hepa1-6 cells were transfected with different plasmids. Twelve hours after transfection, the cells were stimulated with or without 100  $\mu$ M palmitic acid (PA) for 24 h. MTT and colony formation assay were performed as we previously reported.<sup>14,20</sup>

### Tumor xenografts

For one set of experiments, BALB/c nude mice fed with NC or HFD for 8 weeks were subcutaneously injected with  $1 \times 10^6$  HepG2 cells stably expressing either empty vector, or sh*Acs11*, or sh*Aldh2*, or sh*Acs11*+sh*Aldh2*, and mice were maintained on their original diets during the experiment.

For miR-27a-3p agomir and antagomir treatments, nude mice fed with NC or HFD were subcutaneously injected with HepG2 cells and maintained on their original diets. Five micromoles of miR-27a-3p agomir or antagomir or an equal volume of PBS were injected intratumorally every other day at certain times after cell injection, and tumor volume was measured.<sup>20</sup> Detailed protocols are provided in the [supplementary methods](#).

#### qPCR for genes or miRNA and western blots

qPCR (except for miRNA) and western blots were performed as described with details provided in the [supplementary methods](#).<sup>21,22</sup> The primers and antibodies used are provided (Tables S1–2). miRNA levels were evaluated using RiboBio PCR Primer Sets with miR-340-3p as the internal control.

#### Database analysis

The Cancer Genome Atlas (TCGA, <https://cancergenome.nih.gov/>) was used to evaluate the expression of specific genes and miRNAs in patients with HCC and survival rates were calculated using the minimum *p* value approach.<sup>23,24</sup> TargetScan (<http://www.targetscan.org>) was used to predict target genes regulated by miR-27a-3p.

#### Data availability

The RNA-seq data are available at GEO (GSE117539; access token [epxsemamvngxlsj](#)).

#### Statistical analysis

Results were expressed as average  $\pm$  SEM. All of the cell experiments were repeated 3 times. Most data were analyzed using the non-parametric Kruskal-Wallis test followed by the Mann-Whitney *U* test for comparisons of more than 2 groups, while the Mann-Whitney *U* test was used for comparisons of 2 groups. Differences were considered statistically significant when *p* < 0.05.

## Results

### Maternal multigenerational HFD exposure increases HCC incidence in offspring

Compared with the HFD1D and NCD groups, the survival rate of the HFD2D and HFD3D groups (HFD(1/2/3)D, (F0/1/2) male offspring under high-fat diet + diethylnitrosamine) was significantly decreased, with no further difference between these 2 groups (Fig. 1A,B). Serum TC and TG levels were significantly higher in the HFD1D and HFD2D groups compared to those of the NCD and NC mice, which were further significantly increased in the HFD3D group (Fig. 1C), indicating that generational HFD stress gradually increased lipotoxicity in offspring. We previously reported that continuous HFD stress resulted in gradually increased offspring body weight over successive generations.<sup>8</sup> However, in this DEN-induced HCC model, the offspring showed no significant body weight change after exposure to multigenerational HFD stress, maybe due to cancer-associated cachexia.<sup>25</sup> However, increased liver weights (Fig. S2B) and steatosis (data not shown) were found in the HFD-fed plus DEN stress groups compared to the NC group. Notably, the number and size of tumors gradually increased in the offspring over generations under HFD plus DEN stress (Fig. 1D). H&E and trichrome staining also confirmed a gradual deterioration in liver pathology in the offspring over generations under HFD plus DEN stress (Fig. 1E–F).

### Maternal multigenerational HFD exposure increases hepatic inflammation and cell proliferation in the offspring after HFD plus DEN challenge

Increased infiltration of immune cells and hepatocyte proliferation are important characteristics for the development of HCC.<sup>26</sup> A gradual increase in the number of F4/80 (marker of macrophage), CD3 (marker for T cells), Ly-6G (marker for neutrophils), and Ki67 (marker for cell proliferation) stained hepatic cells were found in the livers (both tumor and non-tumor parts) of offspring in succeeding generations upon HFD plus DEN stress (Fig. 2A–B). Markers of liver injury, such as serum AST and ALT, also gradually increased in the offspring over generations (Fig. 2C). Meanwhile, the serum level of AFP, an HCC diagnosis marker,<sup>26,27</sup> was increased in the NCD, HFD1D and HFD2D groups compared to that of the NC mice, which was further increased in the HFD3D mice (Fig. 2D). Also, serum levels of inflammation makers IL-6 and TNF $\alpha$ <sup>28</sup> were increased in NCD mice compared to NC mice, and further increased in the HFD2D and HFD3D groups (Fig. 2D).

### Metabolic genes altered over generations

To explore how multigenerational maternal HFD exposure increases the incidence of HCC in offspring after HFD plus DEN stress, RNA-sequencing for tumors was performed. Among the top 10 KEGG pathways associated with significantly altered genes between different groups (HFD1D vs. HFD3D, NCD vs. HFD3D, NCD vs. HFD1D, HFD1D vs. HFD2D, and HFD2D vs. HFD3D), most were involved in metabolism (Fig. 3A and Fig. S3A–D). Further analysis of the enriched genes in metabolic pathways indicated that most of these genes were down-regulated and belonged to lipid and/or amino acid metabolism (Fig. 3B–C). Consistent with the RNA-sequencing results, qPCR confirmed that in tumors, the levels of *Aldh2*, *Acs11*, *Apoa5*, *Apol7a*, *Rbp4*, *Akr1c6*, *Acaa2*, *Acaa1b*, *Glul*, *Car3*, *Hamp* and *Hamp2* gradually decreased in the livers of offspring in succeeding generations under HFD plus DEN stress (Fig. 3D); meanwhile, similar patterns of changes for these genes were found in non-tumor parts (Fig. S3E), although most of these genes showed significant changes in the HFD2D and HFD3D groups, but not in the HFD1D group (Fig. S3E). Among these genes, we focused on *Acs11* and *Aldh2*, since their levels were significantly negatively correlated with HCC on TCGA analysis (Fig. 3E). Furthermore, patients with HCC and lower *Acs11* or *Aldh2* levels had worse overall survival rates (Fig. 3F). In addition, the levels of *Apoa5*, *Acaa2*, and *Hamp* were also significantly negatively correlated with HCC, while only *Apoa5* and *Hamp* were significantly related to survival rates (Fig. S4). We thus tested whether *Acs11* and *Aldh2* play roles in the increased HCC incidence in offspring.

### Knockdown of *Acs11* and *Aldh2* synergistically promotes tumor growth upon HFD

We individually or simultaneously knocked down *Acs11* and *Aldh2* in HepG2 cells (Fig. S5A). Under normal or PA-treated conditions, both MTT and plate colony formation indicated increased cell proliferation after single or double knockdown of *Acs11* and *Aldh2* (Fig. S5B–C). Interestingly, under PA-treatment, simultaneous knockdown of *Acs11* and *Aldh2* significantly induced cell proliferation compared with knockdown of either gene (Fig. S5B–C), suggesting that they affect cell proliferation synergistically under hyperlipidemic conditions.

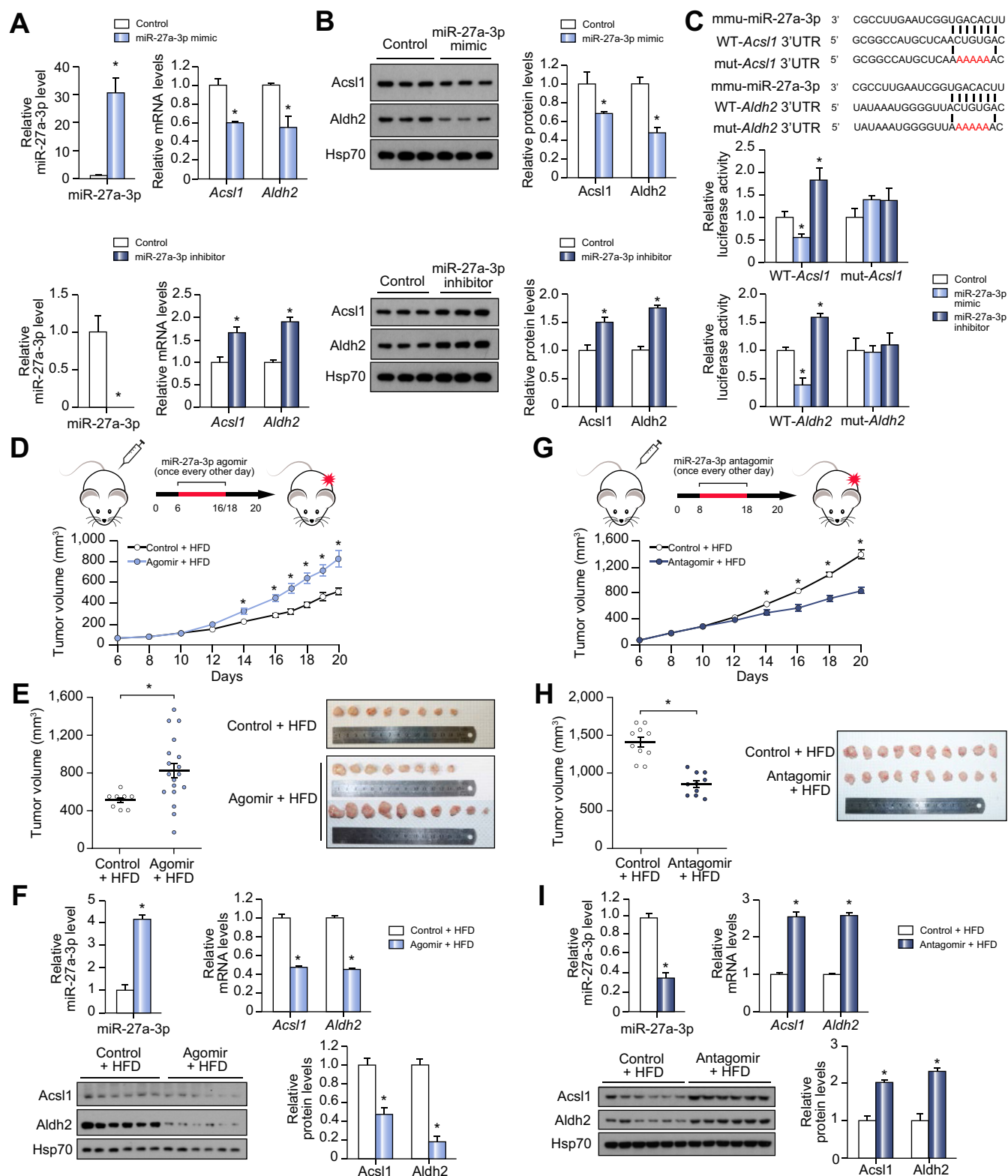


**Fig. 6. miR-27a-3p regulates the expression of *Acsl1* and *Aldh2* and affects cell proliferation.** (A) qPCR results of miR-27a-3p, *Acsl1* and *Aldh2* expression in HepG2 cells following transfection of miR-27a-3p mimic or inhibitor. Data shown as mean  $\pm$  SEM.  $n = 3$  per group;  $*p < 0.05$  (Mann-Whitney *U* test). (B) Western blot results of *Acsl1* and *Aldh2* in HepG2 cells following transfection of miR-27a-3p mimic or inhibitor. Data shown as mean  $\pm$  SEM.  $n = 3$  per group;  $*p < 0.05$  (Mann-Whitney *U* test). (C) Reporter activity for the 3'UTR of wild-type or mutant *Acsl1* and *Aldh2* in the presence of miR-27a-3p mimic or inhibitor. Data shown as mean  $\pm$  SEM.  $n = 4$  per group;  $*p < 0.05$  (Mann-Whitney *U* test). (D, G) Experimental design flowcharts of intratumor injection with the growth curve of xenograft tumor of miR-27a-3p agomir treatment (D; CT,  $n = 8$ ; agomir,  $n = 18$ ), or miR-27a-3p antagonist treatment (G;  $n = 10$  per group) of nude mice under HFD-fed conditions. Data shown as mean  $\pm$  SEM.  $*p < 0.05$  (Mann-Whitney *U* test). (E, H) Volume and picture of xenograft tumor treated with miR-27a-3p agomir

To investigate whether knockdown of *Acsl1* or/and *Aldh2* can exacerbate tumor growth *in vivo*, subcutaneous xenografts were performed. We generated HepG2 cells that stably express sh*Acsl1*, or sh*Aldh2*, or sh*Acsl1*+sh*Aldh2*. Before xenograft injection, nude mice were fed NC or HFD for 8-weeks; significantly increased body weight, serum TC and TG levels were found in HFD-challenged mice (Fig. 4A). Under NC-fed conditions, compared to the control group (CT, injected with HepG2 cells stably expressing empty vector), significantly increased tumor growth rate and size/weight were found in the sh*Acsl1*, sh*Aldh2* and sh*Acsl1*+sh*Aldh2* groups, and no significant difference was observed among these groups (Fig. 4B–D). However, under the HFD-fed conditions, compared to the CT group, tumor growth rate and size/weight were also increased in the sh*Acsl1* or sh*Aldh2* group, which were further increased in the sh*Acsl1*+sh*Aldh2* group (Fig. 4B–D). Notably, compared to the respective NC-fed group, the HFD-fed group showed significantly increased tumor growth rate, size and weight (Fig. 4B–D).

### Hepatic miRNAs altered over generations

The hepatic miRNA levels in the offspring were also examined by RNA-sequencing. Of the top 10 KEGG pathways enriched by significantly altered miRNAs between different groups (HFD1D vs. HFD3D, NCD vs. HFD3D, NCD vs. HFD1D, HFD1D vs. HFD2D, and HFD2D vs. HFD3D), most are involved in cancer development (Fig. 5A and Fig. S6A–D). A heatmap shows a set of miRNAs that are gradually altered over generations (Fig. 5B). Consistent with the RNA-sequencing results, qPCR confirmed that in tumors, miR-210-3p, miR-223-3p, miR-222-5p, miR-322-5p, miR-34c-5p, miR-27a-3p, miR-21a-5p, miR-486a-5p and miR-532-5p were gradually increased in the offspring (Fig. 5C). Meanwhile, similar patterns with lower levels of change were found for some of these miRNAs in non-tumor tissue (Fig. S6E). TCGA analysis suggested that survival rates were significantly decreased in patients with HCC and higher levels of 5 miRNAs including miR-27a-3p (Fig. 5D & Fig. S7).

Increased miRNA levels are often associated with decreased expression of their targeted genes.<sup>29</sup> Bioinformatic analysis suggests that miR-27a-3p may regulate the transcription of *Acsl1* and *Aldh2* (Fig. S8A–B). A mimic or inhibitor of miR-27a-3p was applied to HepG2 or Hepa1-6 cells, and successful regulation of miR-27a-3p level was achieved (Fig. 6A and Fig. S8C). The mRNA and protein levels of *Acsl1* and *Aldh2* were significantly decreased after mimic treatment, while significantly increased after inhibitor treatment (Fig. 6A–B and Fig. S8D–F).

To assess whether miR-27a-3p regulates the transcription of *Acsl1* or *Aldh2* mRNAs, luciferase reporter assays were performed. Co-transfection of the miR-27a-3p mimic with the wild-type, but not mutant, 3'-UTR of *Acsl1* or *Aldh2*, dramatically reduced their transcriptional levels, as demonstrated by the reduction in luciferase activity; while the miR-27a-3p inhibitor had the opposite effect (Fig. 6C). To further investigate the effect of miR-27a-3p on tumor growth, subcutaneous xenograft experiments were performed. Nude mice fed an HFD for 8-weeks

were subcutaneously injected with HepG2 cells (day 0), then miR-27a-3p agomir was injected into the tumors (from day 6 to day 16/18) once every other day (Fig. 6D). Significantly increased tumor growth rate and size were found in agomir-treated mice (Fig. 6D–E). Significantly upregulated miR-27a-3p, as well as downregulated mRNA and protein levels of *Acsl1*/*Aldh2* in the tumors, was achieved by agomir injection (Fig. 6F). Consistently, a miR-27a-3p antagomir had opposite effects on tumor growth rate and size under both NC or HFD conditions (Fig. 6G–H and Fig. S8G–H). The miR-27a-3p antagomir also had the opposite effect on the mRNA and protein levels of *Acsl1*/*Aldh2* in tumors (Fig. 6I). These data suggest that miR-27a-3p regulates *Acsl1* and *Aldh2*, affecting the development of HCC.

### Increased serum miR-27a-3p level in HFD-fed mothers affects HCC susceptibility in the offspring

Maternal miRNAs have been suggested to affect fetal phenotypes,<sup>11,12</sup> thus, we examined 9 miRNAs (Fig. 5C) in serum from the maternal lineage. Gradually increased serum levels of miR-27a-3p, but not the other miRNAs, was found in the maternal lineage under HFD stress (Fig. 7A and Fig. S9). We hypothesized that altered maternal serum miR-27a-3p levels may affect the level of hepatic miR-27a-3p and its target genes in offspring. To test this possibility, an miR-27a-3p agomir was injected once into adult mice. Significantly increased serum miR-27a-3p was seen at 3 h and 3 days, returning to normal levels at 7 days post-injection (Fig. S10A). Next, an miR-27a-3p agomir was injected into pregnant C57BL/6 mice every other day from E12.5 to E18.5 (Fig. 7B). Significantly upregulated miR-27a-3p and downregulated mRNA and protein levels of *Acsl1* and *Aldh2* were achieved in the fetus and pups by elevating maternal serum miR-27a-3p (Fig. 7C–D and Fig. S10B–C).

Therefore, we hypothesized that altered maternal serum miR-27a-3p levels may affect HCC susceptibility in their offspring. To test this possibility, the miR-27a-3p agomir was injected into pregnant C57BL/6 mice, male offspring were challenged with DEN at p15 and fed with NC or HFD after weaning (Fig. 7B). Notably, regardless of diets, significantly increased tumor numbers were found in the offspring whose mothers were injected with miR-27a-3p agomir; furthermore, heavier tumor burden was found in the offspring under HFD conditions (Fig. 7E–F). H&E and trichrome staining indicated exacerbated hepatic pathological changes in the offspring from mothers injected with miR-27a-3p agomir, while, the most significant changes were found in HFD-fed offspring from agomir-injected mothers (Fig. 7G). Moreover, significantly upregulated hepatic miR-27a-3p level with downregulated mRNA and protein levels of *Acsl1* and *Aldh2* were found in the offspring of agomir-injected mothers (Fig. 7H–I).

### miR-27a-3p is negatively correlated with *Acsl1* and *Aldh2* in HCC patients, with or without fatty liver

To investigate the clinical relevance of miR-27a-3p-*Acsl1*/*Aldh2* axis in HCC, 54 clinical samples (27 fatty

(E; CT, n = 8; agomir, n = 18) or antagomir (H; n = 10 per group) under HFD-fed conditions. Data shown as mean ± SEM. \**p* < 0.05 (Mann-Whitney *U* test). (F, I) qPCR and western blot results for *Acsl1* and *Aldh2* in xenograft tumor injected with miR-27a-3p agomir (F) or antagomir (I) (n = 6 per group, except n = 6 and 5 for CT+HFD and antagomir+HFD group, were used to evaluate the *Acsl1* and *Aldh2* levels) under HFD-fed conditions. Data shown as mean ± SEM. \**p* < 0.05 (Mann-Whitney *U* test). CT, control; HFD, high-fat diet; miRNA, microRNA.

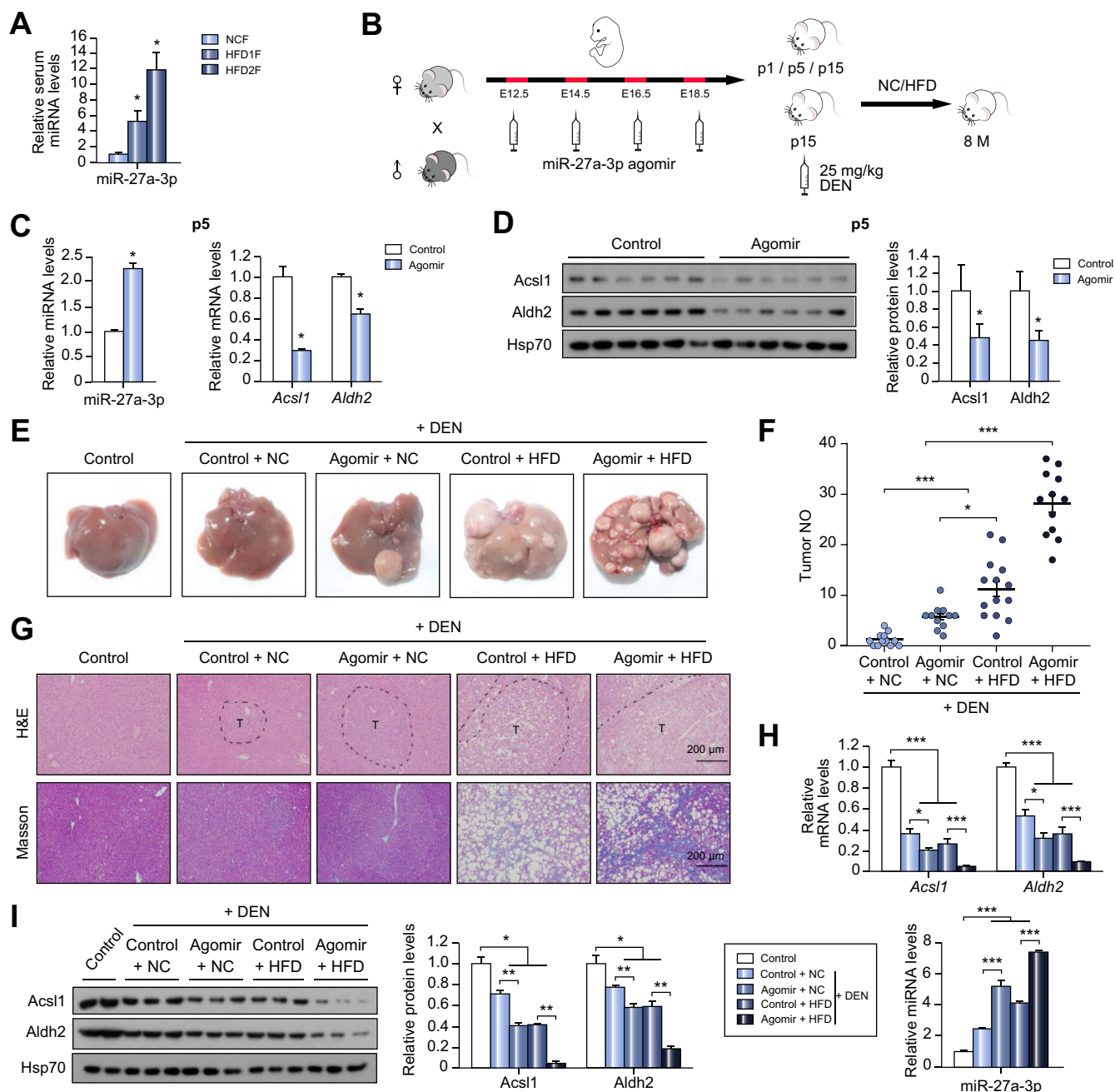


**Fig. 7. Maternal miR-27a-3p level affects the miR-27a-3p-Acs1/Aldh2 level and susceptibility to HCC in their offspring.** (A) qPCR results of miR-27a-3p in the serum of mothers under multigenerational HFD stress. Data shown as mean  $\pm$  SEM.  $n = 4$  per group; \* $p < 0.05$  compared to NC (Mann-Whitney  $U$  test). (B) Experimental flowchart of miR-27a-3p agomir injection to pregnant mice and DEN injection induced HCC in their offspring. (C) qPCR results of miR-27a-3p, Acs1 and Aldh2 in the livers of offspring at p5. Data shown as mean  $\pm$  SEM.  $n = 12$  per group; \* $p < 0.05$  (Mann-Whitney  $U$  test). (D) Western blot results of Acs1 and Aldh2 in the livers of offspring at p5. Data shown as mean  $\pm$  SEM.  $n = 6$  per group; \* $p < 0.05$  (Mann-Whitney  $U$  test). (E-F) Representative liver pictures and quantification results of tumor number (F) for each group. Data shown as mean  $\pm$  SEM.  $n = 12, 11, 14$  and  $12$  for CT+NC, A+NC, CT+HFD and A+HFD group under DEN stress; \* $p < 0.05$ ; \*\*\* $p < 0.001$  (Mann-Whitney  $U$  test). (G) Representative pictures for H&E and Masson stained liver sections ( $n = 4, 5, 5, 5$  and  $5$  for CT+NC without DEN stress, and CT+NC, A+NC, CT+HFD, A+HFD group under DEN stress). Dotted lines indicate the outline of tumors. Scale bar, 200  $\mu$ m. (H) qPCR results of miR-27a-3p, Acs1 and Aldh2 in the livers of offspring. Data shown as mean  $\pm$  SEM.  $n = 8, 10, 10, 10$  and  $10$  for CT+NC without DEN stress, and CT+NC, A+NC, CT+HF, A+HFD group under DEN stress; \* $p < 0.05$ ; \*\*\* $p < 0.001$  (Mann-Whitney  $U$  test). (I) Western blot results of Acs1 and Aldh2 in the livers of offspring. Data shown as mean  $\pm$  SEM.  $n = 3, 6, 6, 6$  and  $6$  for CT+NC without DEN stress, and CT+NC, A+NC, CT+HFD, A+HFD group under DEN stress; \* $p < 0.05$ ; \*\*\* $p < 0.01$  (Mann-Whitney  $U$  test). A, agomir; CT, control; DEN, diethylnitrosamine; HCC, hepatocellular carcinoma; HFD, high-fat diet; miRNA, microRNA; NC, normal chow.

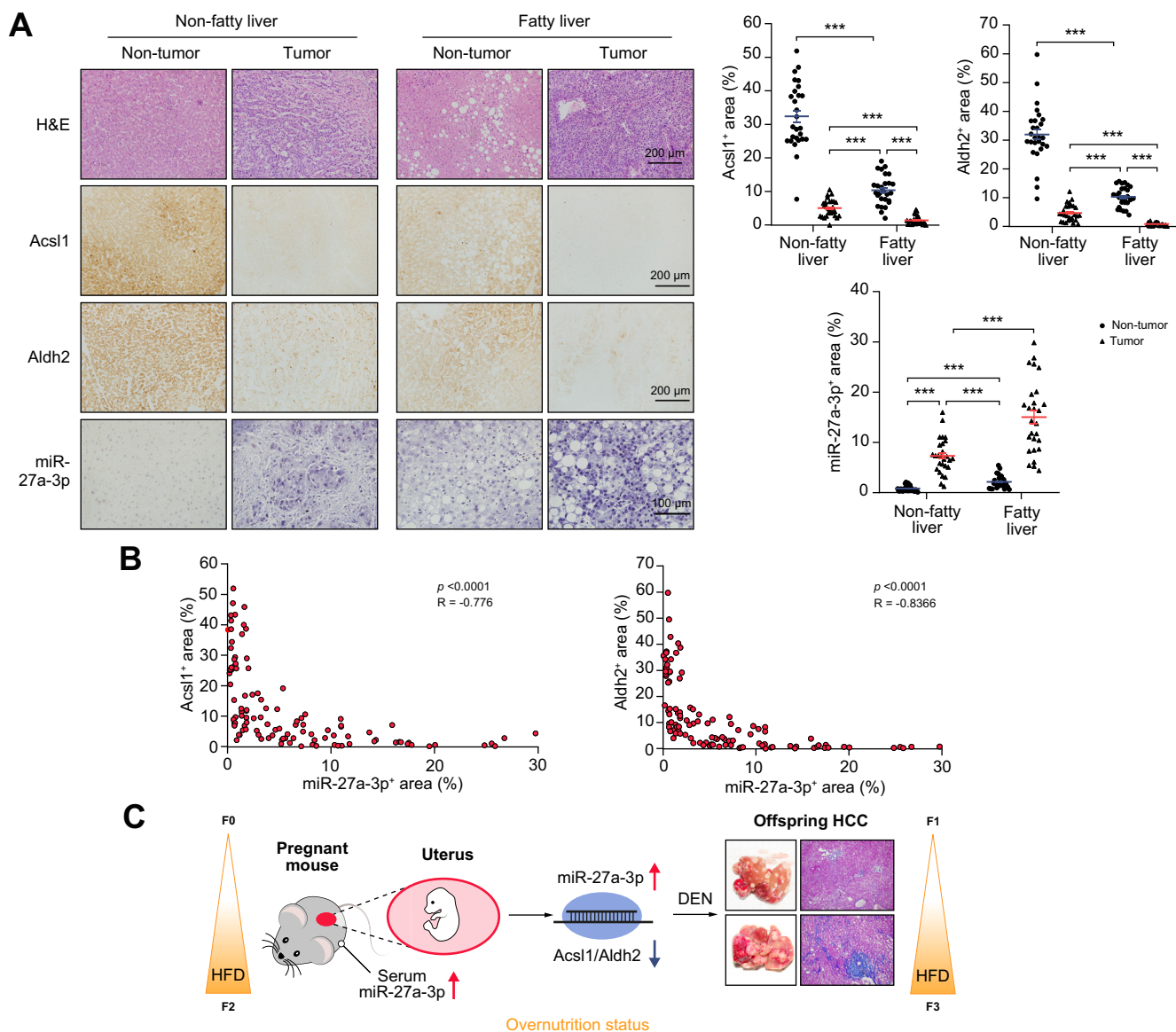


**Fig. 8. Expression level of miR-27a-3p showed negative correlation with Acs1 and Aldh2 in liver of patients with HCC with or without fatty liver.** (A) Representative pictures for H&E, immunohistochemistry of Acs1 and Aldh2, and *in situ* hybridization of miR-27a-3p staining (left) and quantification results (right). Data shown as mean  $\pm$  SEM.  $n = 27$  per group; \*\*\* $p < 0.001$  (Mann-Whitney *U* test). Scale bar, 100 or 200  $\mu$ m. (B) Correlation between expression levels of miR-27a-3p and Acs1, and miR-27a-3p and Aldh2.  $n = 108$ ; data analyzed with spearman correlation analysis. (C) A proposed model for the role of maternal serum miR-27a-3p and the hepatic miR-27a-3p-Acs1/Aldh2 axis in regulating offspring's susceptibility to HCC. DEN, diethylnitrosamine; HCC, hepatocellular carcinoma; HFD, high fat diet; miRNA, microRNA.

liver-associated HCC, 27 non-fatty liver-associated HCC) were obtained. The levels of Acs1 or Aldh2 in tumors were significantly lower compared to those in non-tumor tissues, and their levels in fatty liver samples were also significantly lower compared to those in non-fatty liver (Fig. 8A). Consistently, the miR-27a-3p levels in tumors were significantly higher compared with those in non-tumor tissues, while its levels were significant higher in fatty liver samples compared to those in non-fatty liver (Fig. 8A). Correlation analysis further revealed a negative correlation between the expression of miR-27a-3p and Acs1 or Aldh2 (Fig. 8B).

## Discussion

The present study indicates that maternal obesity affects the incidence and development of HCC in offspring. Specifically, obesity or HFD-feeding increased the maternal serum miR-27a-3p levels, which could intergenerationally affect the hepatic miR-27a-3p-Acs1/Aldh2 axis in offspring (Fig. 8C). Since maternal obesity is an independent contributing factor to metabolic diseases in offspring, and HCC is closely associated with metabolic diseases, our animal studies reveal a mechanistic link between maternal obesity and the development of cancer in offspring. Further clinical and epidemiological investigations will help to link our findings in humans.

Disruption of miRNA expression patterns is regarded as a hallmark of human cancer.<sup>30</sup> Many miRNAs are involved in human cancer as onco-miRNA or tumor suppressor-miRNA, depending on their gene targets.<sup>31,32</sup> miR-27a-3p is upregulated in laryngeal tumors and gastric cancer<sup>33,34</sup>; and its level is correlated with metastatic progression and survival rates in nasopharyngeal carcinoma.<sup>35</sup> Herein, we found that serum miR-27a-3p levels increased over generations in response to obesity in the maternal lineage (Fig. 7A). Interestingly, we also observed elevated hepatic miR-27a-3p levels over generations in the offspring from these obese mothers under HFD plus DEN stress (Fig. 5B–C), which may occur through transportation of miRNAs from mothers to their offspring via small extracellular vesicles.<sup>36,37</sup> Intratumor injection of a miR-27a-3p agomir increased tumor growth rates in nude mice, whereas an antagomir had the opposite effects (Fig. 6D–H and Fig. S8G–H). Notably, injection of pregnant mice with a miR-27a-3p agomir exacerbated DEN-induced HCC development in offspring under NC- and HFD-fed conditions (Fig. 7E–G). In humans, the hepatic miR-27a-3p level was positively correlated with HCC (Fig. 8A) and mortality (Fig. 5D). Although additional miRNAs, such as miR-210-3p and miR-223-3p, may not be responsible for the intergenerational effects observed in the offspring of obese mothers, their roles in HCC development still await further investigation.

In this study, we demonstrated *in vitro* and *in vivo* that *Acs11* and *Aldh2* are targets for miR-27a-3p (Fig. 6). *Acs11* catalyzes the acylation of fatty acids into long-chain acyl-CoAs<sup>38</sup>; whereas *Aldh2* is a mitochondrial aldehyde dehydrogenase highly expressed in the liver,<sup>39</sup> which is involved in normalizing the acetaldehyde-redox level. Downregulated *Aldh2* has been shown to enhance the migratory capacity of HCC in mice.<sup>40</sup> Consistently, we demonstrated gradual decreases of *Aldh2* and *Acs11* in DEN-induced offspring exposed to multigenerational HFD stress (Fig. 3C–D). Additionally, TCGA analysis suggested significantly lower *Aldh2* or *Acs11* levels in patients with HCC, which are also negatively correlated with mortality (Fig. 3E–F). Furthermore, under both NC-fed and HFD-fed conditions, the offspring of agomir-injected pregnant mice showed upregulated hepatic miR-27a-3p, with downregulated hepatic *Aldh2* and *Acs11* levels (Fig. 7). These results demonstrated a novel regulatory role for hepatic miR-27a-3p on *Acs11* and *Aldh2* in the development of HCC.

Double knockdown of *Acs11* and *Aldh2* had a synergistic effect on tumor growth under hyperlipidemic conditions, both *in vivo* and *in vitro*, but not under normal conditions (Fig. 4B–D and Fig. S5B–C). Cancers are complex diseases with heterogeneous genetic causes,<sup>41</sup> in many cases, multiple mutations and/or gene loss contribute to cell proliferation, differentiation and cellular homeostasis during cancer development.<sup>42</sup> Thus, the synergistic effects of *Acs11* and *Aldh2* on tumor growth may be due to co-ordination of multiple signaling pathways and the provision of metabolic substrates during cancer development.<sup>43</sup> Whether this synergistic effect takes place under other conditions requires further investigation.

In summary, an important link between maternal obesity and diseases in offspring has been described. Attention should be paid to the potential clinical impacts of intergenerational and multigenerational phenomena.

## Abbreviations

AFP, alpha-fetoprotein; ALT, alanine aminotransferase; AST, aspartate aminotransferase; CT, control; DEN, diethylnitrosamine; HCC, hepatocellular carcinoma; HFD, high-fat diet; HFD(1/2/3)D, (F0/1/2) male offspring under high-fat diet + DEN; IL-, interleukin; miRNA, microRNA; NAFLD, non-alcoholic fatty liver disease; NC, normal chow; NCD, normal chow + DEN; PA, palmitic acid; shRNA, short hairpin RNA; TC, total cholesterol; TCGA, The Cancer Genome Atlas; TG, triglyceride; TNF $\alpha$ , tumor necrosis factor- $\alpha$ .

## Financial support

This work is supported by the National Key R&D Program of China (2018YFA0800700 & 2019YFA0802701), the Natural Science Foundation of China (91957114, 31871381, 31671195, 31971066 & 31871411).

## Conflict of interest

The authors declare no competing interests.

Please refer to the accompanying ICMJE disclosure forms for further details.

## Authors' contributions

Y.S. K.H., L.Z. designed research; Y.S., Q.W., Y.Z., M.G., Y.W., Y.L., S.L., J.Y. performed experiments; Y.S., R.B.P., K.H., L.Z. analyzed data; K.H., L.Z. wrote the manuscript.

## Supplementary data

Supplementary data to this article can be found online at <https://doi.org/10.1016/j.jhep.2020.03.050>.

## References

Author names in bold designate shared co-first authorship

- [1] Calle EE, Kaaks R. Overweight, obesity and cancer: epidemiological evidence and proposed mechanisms. *Nat Rev Cancer* 2004;4:579–591.
- [2] Bugianesi E. Non-alcoholic steatohepatitis and cancer. *Clin Liver Dis* 2007;11:191–207.
- [3] Calle EE, Rodriguez C, Walker-Thurmond K, Thun MJ. Overweight, obesity, and mortality from cancer in a prospectively studied cohort of U.S. adults. *N Engl J Med* 2003;348:1625–1638.
- [4] Siegel AB, Zhu AX. Metabolic syndrome and hepatocellular carcinoma: two growing epidemics with a potential link. *Cancer* 2009;115:5651–5661.
- [5] O'Reilly JR, Reynolds RM. The risk of maternal obesity to the long-term health of the offspring. *Clin Endocrinol* 2013;78:9–16.
- [6] Catalano PM, Ehrenberg HM. The short- and long-term implications of maternal obesity on the mother and her offspring. *BJOG* 2006;113:1126–1133.
- [7] Frantz ED, Aguila MB, Pinheiro-Mulder Ada R, Mandarim-de-Lacerda CA. Transgenerational endocrine pancreatic adaptation in mice from maternal protein restriction in utero. *Mech Ageing Dev* 2011;132:110–116.
- [8] Li J, Huang J, Li JS, Chen H, Huang K, Zheng L. Accumulation of endoplasmic reticulum stress and lipogenesis in the liver through generational effects of high fat diets. *J Hepatol* 2012;56:900–907.
- [9] Martinez JA, Cordero P, Campion J, Milagro FI. Interplay of early-life nutritional programming on obesity, inflammation and epigenetic outcomes. *Proc Nutr Soc* 2012;71:276–283.
- [10] Nelson VR, Nadeau JH. Transgenerational genetic effects. *Epigenomics* 2010;2:797–806.
- [11] **Li J, Zhang Y**, Li D, Liu Y, Chu D, Jiang X, et al. Small non-coding RNAs transfer through mammalian placenta and directly regulate fetal gene expression. *Protein Cell* 2015;6:391–396.

- [12] Floris I, Kraft JD, Altosaar I. Roles of microRNA across prenatal and postnatal periods. *Int J Mol Sci* 2016;17:E1994.
- [13] Ding Y, Li J, Liu S, Zhang L, Xiao H, Li J, et al. DNA hypomethylation of inflammation-associated genes in adipose tissue of female mice after multigenerational high fat diet feeding. *Int J Obes* 2014;38:198–204.
- [14] Liu S, Sun Y, Jiang M, Li Y, Tian Y, Xue W, et al. Glyceraldehyde-3-phosphate dehydrogenase promotes liver tumorigenesis by modulating phosphoglycerate dehydrogenase. *Hepatology* 2017;66:631–645.
- [15] Chen H, Huang Y, Zhu X, Liu C, Yuan Y, Su H, et al. Histone demethylase UTX is a therapeutic target for diabetic kidney disease. *J Physiol* 2019;597:1643–1660.
- [16] Zhang Y, Xue W, Zhang W, Yuan Y, Zhu X, Wang Q, et al. Histone methyltransferase G9a protects against acute liver injury through GSTP1. *Cell Death Differ* 2020;27:1243–1258.
- [17] Liu X, Li Y, Meng L, Liu XY, Peng A, Chen Y, et al. Reducing protein regulator of cytokinesis 1 as a prospective therapy for hepatocellular carcinoma. *Cell Death Dis* 2018;9:534.
- [18] Wang W, Wang Q, Wan D, Sun Y, Wang L, Chen H, et al. Histone HIST1H1C/H1.2 regulates autophagy in the development of diabetic retinopathy. *Autophagy* 2017;13:941–954.
- [19] Zhang Y, Guo X, Yan W, Chen Y, Ke M, Cheng C, et al. ANGPTL8 negatively regulates NF-kappaB activation by facilitating selective autophagic degradation of IKKgamm. *Nat Commun* 2017;8:2164.
- [20] Liu X, Zhou Y, Liu X, Peng A, Gong H, Huang L, et al. MPHOSPH1: a potential therapeutic target for hepatocellular carcinoma. *Cancer Res* 2014;74:6623–6634.
- [21] Chen H, Wang L, Wang W, Cheng C, Zhang Y, Zhou Y, et al. ELABELA and an ELABELA fragment protect against AKI. *J Am Soc Nephrol* 2017;28:2694–2707.
- [22] Xue W, Huang J, Chen H, Zhang Y, Zhu X, Li J, et al. Histone methyltransferase G9a modulates hepatic insulin signaling via regulating HMG A1. *Biochim Biophys Acta Mol Basis Dis* 2018;1864:338–346.
- [23] Cui K, Liu C, Li X, Zhang Q, Li Y. Comprehensive characterization of the rRNA metabolism-related genes in human cancer. *Oncogene* 2020;39:786–800.
- [24] Hirata H, Sugimachi K, Komatsu H, Ueda M, Masuda T, Uchi R, et al. Decreased expression of fructose-1,6-bisphosphatase associates with glucose metabolism and tumor progression in hepatocellular carcinoma. *Cancer Res* 2016;76:3265–3276.
- [25] Petruzzelli M, Schweiger M, Schreiber R, Campos-Olivas R, Tsoli M, Allen J, et al. A switch from white to brown fat increases energy expenditure in cancer-associated cachexia. *Cell Metab* 2014;20:433–447.
- [26] El-Serag HB. Hepatocellular carcinoma. *N Engl J Med* 2011;365:1118–1127.
- [27] Song PP, Xia JF, Inagaki Y, Hasegawa K, Sakamoto Y, Kokudo N, et al. Controversies regarding and perspectives on clinical utility of biomarkers in hepatocellular carcinoma. *World J Gastroenterol* 2016;22:262–274.
- [28] Park EJ, Lee JH, Yu GY, He G, Ali SR, Holzer RG, et al. Dietary and genetic obesity promote liver inflammation and tumorigenesis by enhancing IL-6 and TNF expression. *Cell* 2010;140:197–208.
- [29] Ma R, Wang C, Wang J, Wang D, Xu J. miRNA-mRNA interaction network in non-small cell lung cancer. *Interdiscip Sci Comput Life Sci* 2016;8:209–219.
- [30] Yang LH, Dong Z, Gong ZH. Extracellular miRNA: a novel molecular biomarker for lung cancer. *Yi Chuan* 2012;34:651–658.
- [31] Sun J, Lu H, Wang X, Jin H. MicroRNAs in hepatocellular carcinoma: regulation, function, and clinical implications. *Scientific World J* 2013;2013:924206.
- [32] Lu J, Getz G, Miska EA, Alvarez-Saavedra E, Lamb J, Peck D, et al. MicroRNA expression profiles classify human cancers. *Nature* 2005;435:834–838.
- [33] Zhou L, Liang X, Zhang L, Yang L, Nagao N, Wu H, et al. MiR-27a-3p functions as an oncogene in gastric cancer by targeting BTG2. *Oncotarget* 2016;7:51943–51954.
- [34] Tian Y, Fu S, Qiu GB, Xu ZM, Liu N, Zhang XW, et al. MicroRNA-27a promotes proliferation and suppresses apoptosis by targeting PLK2 in laryngeal carcinoma. *BMC Cancer* 2014;14:678.
- [35] Li L, Luo Z. Dysregulated miR-27a-3p promotes nasopharyngeal carcinoma cell proliferation and migration by targeting Mapk10. *Oncol Rep* 2017;37:2679–2687.
- [36] Zhang Y, Liu D, Chen X, Li J, Li L, Bian Z, et al. Secreted monocytic miR-150 enhances targeted endothelial cell migration. *Mol Cell* 2010;39:133–144.
- [37] Rodosthenous RS, Burris HH, Sanders AP, Just AC, Dereix AE, Svensson K, et al. Second trimester extracellular microRNAs in maternal blood and fetal growth: an exploratory study. *Epigenetics* 2017;12:804–810.
- [38] Li LO, Ellis JM, Paich HA, Wang S, Gong N, Altshuler G, et al. Liver-specific loss of long chain acyl-CoA synthetase-1 decreases triacylglycerol synthesis and beta-oxidation and alters phospholipid fatty acid composition. *J Biol Chem* 2009;284:27816–27826.
- [39] Muzio G, Maggiora M, Paiuzzi E, Oraldi M, Canuto RA. Aldehyde dehydrogenases and cell proliferation. *Free Radic Biol Med* 2012;52:735–746.
- [40] Hou G, Chen L, Liu G, Li L, Yang Y, Yan HX, et al. Aldehyde dehydrogenase-2 (ALDH2) opposes hepatocellular carcinoma progression by regulating AMP-activated protein kinase signaling in mice. *Hepatology* 2017;65:1628–1644.
- [41] Zhong X, Yang H, Zhao S, Shyr Y, Li B. Network-based stratification analysis of 13 major cancer types using mutations in panels of cancer genes. *BMC Genomics* 2015;16(Suppl 7):S7.
- [42] Guo XE, Ngo B, Modrek AS, Lee WH. Targeting tumor suppressor networks for cancer therapeutics. *Curr Drug Targets* 2014;15:2–16.
- [43] Iurlaro R, Leon-Annicchiarico CL, Munoz-Pinedo C. Regulation of cancer metabolism by oncogenes and tumor suppressors. *Methods Enzymol* 2014;542:59–80.